Synthesis, Characterization, and Kinetic of Thermal Degradation of Oligo-2-[(4-bromophenylimino)methyl]phenol and Oligomer-Metal Complexes

İsmet Kaya, Ahmet Solguntekin

Department of Chemistry, Faculty of Sciences and Arts, Çanakkale Onsekiz Mart University, Çanakkale TR 17020, Turkey

Received 8 January 2008; accepted 15 February 2009
DOI 10.1002/app.30272
Published online 17 April 2009 in Wiley InterScience (www.interscience.wiley.com).

ABSTRACT: Oligo-2-[(4-bromophenylimino)methyl]phenol (OBPIMP) was synthesized from the oxidative polycondensation reaction of 2-[(4-bromophenylimino)methyl] phenol (BPIMP) with air and NaOCl oxidants in an aqueous alkaline medium between 50 and 90°C. The yield of OBPIMP was found to be 67 and 88% for air and NaOCl oxidants, respectively. Their structures were confirmed by elemental and spectral such as IR, ultraviolet–visible spectrophotometer (UV–vis), ^{1}H-NMR, and ^{13}C-NMR analyses. The characterization was made by TG-DTA, size exclusion chromatography, and solubility tests. The resulting complexes were characterized by electronic and IR spectral measurements, elemental analysis, AAS, and thermal studies. According to TG analyses, the weight losses of OBPIMP, and oligomer-metal complexes with Co^{+2}, Ni^{+2}, and Cu^{+2} ions were found to be 93.04%, 59.80%, 74.23%, and 59.30%, respectively, at 1000°C. Kinetic and thermodynamic parameters of these compounds investigated by Coats-Redfern, MacCallum-Tanner, and van Krevelen methods. The values of the apparent activation energies of thermal decomposition (E_a), the reaction order (n), preexponential factor (A), the entropy change (ΔS^*), enthalpy change (ΔH^*), and free energy change (ΔG^*) obtained by earlier-mentioned methods were all good in agreement with each other. It was found that the thermal stabilities of the complexes follow the order Cu(II) > Co(II) > Ni(II).
 J Appl Polym Sci 113: 1994–2007, 2009

Key words: azomethine oligomer; kinetic of thermal degradation; oxidative polycondensation; oligomer-metal complexes

INTRODUCTION

Research interest in polyazomethines continues because of their different characteristics such as chelating properties,[1,2] thermal stability,[3,4] liquid crystal properties,[5–9] and intrinsic conductivity[7]. Polyazomethines are generally synthesized by polycondensation reactions, a method that has some disadvantages, among them being the necessity to ensure special reaction conditions (such as high temperature) and the use, in some cases, of special catalysts.[10] There are some significant advantages of this method because of using of oxidants such as NaOCl, H_2O_2, and air. For example, these type oxidants are cheap and easily provided. Phenols and Schiff base substitute phenols were polymerized at easy a form by using these oxidants.[11] With a view to searching for potential materials for electric, magnetic, and optical application, our group has been working at the synthesis of Schiff base substitute oligophenol and their metal complexes in recent years. Azomethine polymer or oligomers including conjugated bonding and active hydroxyl group have been studied for more than 60 years and they have been used in various fields. They have useful properties such as paramagnetism, semi conductivity, electrochemical cell, and resisting to high energy. Because of these properties, they are used to prepare composites having high resistance at high temperature, thermo-stabilisatiors, graphite materials, and epoxy oligomer and block copolymers, photo resists, materials which are antistatic and enduring to flame.[12–20] Addition of functional groups to these compounds can lead to new or enhanced properties. Schiff bases polymers, for instance, have demonstrated antimicrobial activities against various bacteria, yeast, and fungus. Azomethine polymers or oligomers having many functional groups have utility for scrubbing poisonous heavy metals from industrial waste waters. Therefore, the synthesis of oligomer-metal complexes is very important in analytic and environmental chemistry. It seemed advantageous to attempt to design and prepare a polymer-bound chelating ligand, which would be able to form complexes with

Correspondence to: İ. Kaya (kayaismet@hotmail.com).

a variety of transition metals and therefore have a large range of applications.[21]

Kinetics methods

Non-isothermal methods have been extensively used for the study of the kinetics and mechanism of condensed phase reactions.[22] In general, most methods of kinetic analysis of thermo analytical data begin with the Arrhenius' equation,

$$k = A\,e^{(-E_a/RT)} \tag{1}$$

and a rate expression

$$\frac{d\alpha}{dt} = kf(\alpha) \tag{2}$$

In eq. (2), $f(\alpha)$ is a so-called kinetic function that depends on the reaction mechanism, where α represents the fractional conversion (increasing from 0 to 1) in the solid reactant during the course of the reaction, If $f(\alpha) = (1 - \alpha)^n$ and with a constant temperature increase, $dT/dt = \beta$, (β is the heating rate in °C/min) integration of eq. (2) leads to

$$g(\alpha) = \int_0^{\alpha} \left[\frac{1}{(1-\alpha)^n}\right] d\alpha = \frac{A}{\beta} \int_{T_0}^{T} \exp\left(\frac{-E_a}{RT}\right) dT \tag{3}$$

where n is reaction order, For the special case $n = 1$,

$$\int_0^{\alpha} \left[\frac{1}{(1-\alpha)^n}\right] d\alpha = -\ln(1-\alpha) \tag{4}$$

For n not equal to zero or unity

$$\int_0^{\alpha} \left[\frac{1}{(1-\alpha)^n}\right] d\alpha = -\frac{1-(1-\alpha)^{1-n}}{1-n} \tag{5}$$

Several techniques using different approaches have been developed to solve the integral of eq. (3). The three methods investigated in this article are Coats-Redfern method (CR), MacCallum-Tanner method (MC), and van Krevelen method (vK).

The CR method

The following equation can be obtained with using an asymptotic approximation for resolution of eq. (3):

$$\ln\left[\frac{g(\alpha)}{T^2}\right] = \ln\left[\frac{AR}{\beta E_a}\left(1 - \frac{2RT}{E_a}\right)\right] - \left(\frac{E_a}{RT}\right) \tag{6}$$

The authors[23] supposed that $\ln\left(1 - \frac{2RT}{E_a}\right) \to 0$ for the Doyle approximation,[24] obtaining in natural logarithmic form:

$$\ln g(\alpha) \cong \ln\left[\frac{AR}{\beta E_a}\right] - \frac{E_a}{RT}$$

The apparent activation energy of thermal decomposition for each decomposition mechanisms can be obtained from the slope of a plot of $\ln[g(\alpha)/T^2]$ versus $1000/T$.

The MC method

The method by MacCallum and Tanner[25] provides an approximation integrated from the rate of degradation as a function of temperature. The rate of degradation can be thus expressed by:

$$\log g(\alpha) = \log\frac{AE_a}{\beta R} - 0.4828E^{0.4351} - \left(\frac{0.449 + 0.217E_a}{10^{-3}T}\right) \tag{7}$$

A plot of $\log g(\alpha)$ versus $1/T$ can give E from the slope, and A from the intersection of the Y axis.

The vK method

The integration method used by van Krevelen[26] is expressed as:

$$n \neq 1 \quad \ln g(\alpha) = \ln\left[\frac{A(0.368/T_m)^x}{\beta(x+1)}\right] + (x+1)\ln T \tag{8}$$

where $x = E_a/RT_m$, and T_m is the temperature at the maximum rate of weight loss. Therefore, E can be obtained from the slope of a plot of $\ln\, g(\alpha)$ versus $\ln\, T$. In the earlier equations, $g(\alpha)$, β, T_m, E_a, A, R, k are the integral function of conversion, heating rate, DTG peak temperature, the apparent activation energy of thermal decomposition (kJ mol^{-1}), pre-exponential factor (min^{-1}), gas constant (8.314 J mol^{-1} K^{-1}), and specific rate constant, respectively. The kinetic parameters were calculated from the linear plots of the left-hand side of kinetic equations [eqs. (6) and (7)] against $1/T$, for van Krevelen equation [eq. (8)] the left-hand side is plotted against $\ln T$. The values E_a and A were calculated from the slope and intercept of the straight lines, respectively.

In this article, we have investigated the effects of different parameters such as temperature, initial concentration of NaOCl and alkaline for the preparation of oligo-2-[(4-bromophenylimino) methyl]phenol, and then we determined optimum reaction conditions by oxidative polycondensation method for BPIMP. The BPIMP and OBPIMP were characterized by using FTIR, UV–vis, ^{1}H-^{13}C-NMR, elemental analysis, and size exclusion chromatography (SEC) techniques. Besides, oligomer-metal complexes were

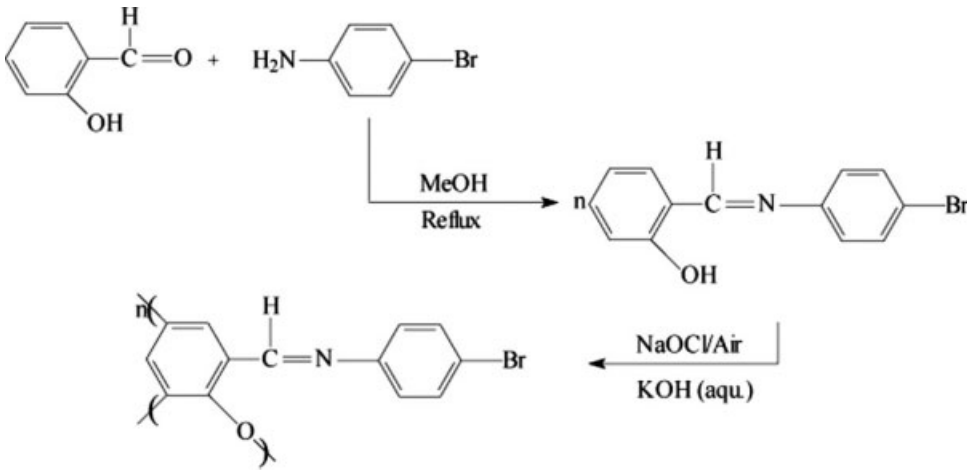

Scheme 1 Syntheses of monomer and oligomer.

synthesized from the reactions of OBPIMP with Co(II), Ni(II), and Cu(II) acetates. Also, thermal stabilities of OBPIMP and oligomer-metal complexes were studied by TGA-DTA techniques. The kinetic and thermodynamic parameters of thermal degradation of monomer, oligomer, and oligomer-metal complexes were investigated by various methods of TG analyses.

EXPERIMENTAL

Materials

Salicylaldehyde (SA), 4-bromo-aniline (4-BrA), methanol, ethanol, benzene, acetone, toluene, heptane, hexane, tetrahydrofurane, THF, *N, N′*-dimethylformamide, DMF, dimethylsulfoxide, DMSO, H_2SO_4, NaOH, KOH, hydrochloric acid (HCl, 37%), $Cu(CH_3COO)_2$ H_2O, $Co(CH_3COO)_2$ $4H_2O$, and $Ni(CH_3COO)_2$ $4H_2O$ were supplied from Merck Chemical (Germany) and they were used as received. Sodium hypo chlorite, (NaOCl, 30%, aqueous solution) was supplied from Paksoy (Turkey).

Synthesis of 2-[(4-bromophenylimino)methyl]phenol

4-BrA (0.025 mol) and SA (0.025 mol) were dissolved in methanol (MeOH) (15 mL) and placed into a 50-mL two-necked round-bottom flask (Scheme 1). It was fitted with a condenser and thermometer. The mixture was stirred magnetically on a water bath at 70°C for 3 h. The precipitated 2-[(4-bromophenylimino)methyl]phenol was filtered, recrystallized from MeOH and dried in a vacuum desiccator (yield 94%).

Calcd. for BPIMP: C, 56.54; H, 3.62; N, 5.07. Found: C, 56.25; H, 3.30; N, 4.90. FTIR (KBr; cm^{-1}): *v*(CH=N) 1610 s, *v*(C—O) 1282 s, *v*(C=C) 1569, 1481, 1452, 1407 s, *v*(aromatic C—H) 3057 s, *v*(Ar—OH) 3346 s, *v*(C—Br) 753 s. UV–vis (λ_{max}): 211, 230, 273, 320, and 341 nm. ^{1}H-NMR (DMSO): δ ppm, 12.80 (s, 1H, OH), 8.95 (s, 1H, CH=N), 7.64 (d, 2H, Ar—Haa′), 7.38 (d, 2H, Ar—Hbb′), 7.67 (d, 1H, Ar—Hc), 7.02 (m, 1H, Ar—Hd), 7.45 (m, 1H, Ar—He), 6.98 (d, 1H, Ar—Hf). ^{13}C-NMR (DMSO): δ ppm, 163.54 (C1-ipso), 116.35 (C2), 133.60 (C3), 123.18 (C4), 131.94 (C5), 118.92 (C6-ipso), 165.18 (C7), 147.88 (C8-ipso), 124.85 (C9), 131.89 (C10), 120.54 (C11).

Synthesis of oligo-2-[(4-chlorophenyl) iminomethylene]phenol with NaOCl and air oxidants in aqueous alkaline medium

OBPIMP was synthesized through oxidative polycondensation of 2-[(4-chlorophenyl)imino methylene]phenol with aqueous solutions of NaOCl (30%) and air, respectively.[27] The BPIMP (0.200 g, 7.25×10^{-4} mol) was dissolved in an aqueous solution of KOH (0.400 g, 1.45×10^{-3} mol) and placed into a 50 mL three-necked round-bottom flask (Scheme 1). It was fitted with a condenser, thermometer, stirrer, and an addition funnel containing NaOCl. After heating to 40°C, NaOCl was added drop by drop over about 20 min. The reaction mixtures were stirred at the various temperatures and durations (Table I). Alternatively, the air was passed into an aqueous solution of KOH (20%) before passage through the reaction tube to prevent water loss in the reaction mixture and remove CO_2. The reaction mixtures were cooled to room temperature, and then 1.45×10^{-3} mol HCl (37%) was added. Unreacted monomer was separated from the reaction products by washing with MeOH. The mixture was filtered and washed with hot water (3×25 mL) to remove mineral salts and then dried in an oven at 105°C.

Calcd. for OBPIMP: C, 56.95; H, 2.92; N, 5.11. Found: C, 65.84; H, 3.70; N, 5.85. FTIR (KBr, cm^{-1}):

TABLE I
The Oxidative Polycondensation of 2-[(4-bromophenylimino)methyl]phenol[a] Using NaOCl (Sample No: 1–17) and Air (Sample No: 18–25) in an Aqueous KOH

Sample no.	$[KOH]_0$ (mol L^{-1})	$[NaOCl]_0$ (mol L^{-1})/ Air (L/h)	Temp. (°C)	Time (h)	Yield of OBPIMP (%)
1	0.06	0.03	50	5	67
2	0.06	0.03	60	5	45
3	0.06	0.03	70	5	60
4	0.06	0.03	80	5	50
5	0.06	0.03	90	5	45
6	0.06	0.03	50	1	71
7	0.06	0.03	50	2	88
8	0.06	0.03	50	3	68
9	0.06	0.03	50	4	66
10	0.06	0.03	50	5	67
11	0.06	0.03	50	10	43
12	0.06	0.03	50	20	48
13	0.06	0.06	50	5	69
14	0.06	0.06	60	5	60
15	0.06	0.06	70	5	53
16	0.06	0.06	80	5	51
17	0.06	0.06	90	5	45
18	0.06	8.5	50	5	67
19	0.06	8.5	60	5	35
20	0.06	8.5	70	5	21
21	0.06	8.5	80	5	11
22	0.06	8.5	90	5	17
23	0.06	8.5	50	3	52
24	0.06	8.5	50	10	34
25	0.06	8.5	50	20	30

[a] The initial concentration of BPIMP was used as 0.03 mol L^{-1}.

ν(O—H) 3428 s, ν(C—H aryl) 3070 m, ν(C=N) 1617 s, ν(aromatic, C—O) 1282 s, ν(C—Br) 755 s, ν(aromatic, C=C) 1586, 1485, 1458 m. UV–vis (λ_{max}): 240, 288, 330 and 354 nm. ^{1}H-NMR (DMSO): δ ppm, 12.82 (s, 1H, OH), 8.97 (s, 1H, CH=N), 7.64 (d, 2H, Ar—Haa′), 7.42 (d, 2H, Ar—Hbb′), 7.68 (s, 1H, Ar-Hc), 6.99 (d, 1H, Ar-Hd), 7.46 (s, 1H, Ar-He), 6.97 (d, 1H, Ar-Hf). ^{13}C-NMR (DMSO): δ ppm, 164.46 (C1-ipso), 118.42 (C2-ipso), 133.78 (C3), 123.25 (C4), 132.02 (C5), 119.30 (C6-ipso), 167.54 (C7), 149.25 (C8-ipso), 124.56 (C9), 132.44 (C10), 120.61 (C11); 121.93 new peak.

Syntheses of oligo-2-[(4-bromophenylimino) methyl] phenol-metal complexes

Cobalt (II) complex

A solution of $Co(AcO)_2$ $4H_2O$ (0.250 g, 7.5×10^{-4} mol) in MeOH (10 mL) was added to a solution of OBPIMP (0.500 g, 1.8×10^{-3} mol/unit) in THF (20 mL). The mixture was stirred and heated at 70°C for 5 h (Scheme 2) and the precipitated complex was filtered off, washed with cold MeOH/THF, and dried in vacuum oven (yield 69%).

Calcd. for OBPIMP-Co: M, 17.70. Found: M, 12.00. UV–vis (λ_{max}): 206, 237, 281, 343, and 383 nm. FTIR (KBr, cm^{-1}): ν(O—H) 3447 s, ν(C—H aryl) 3057 m, ν(C=N) 1603 s, ν(aromatic, C—O) 1172 s, ν(C—Br) 826 s, ν(aromatic, C=C) 1589, 1576, 1528, 1460 m, ν(M—O) 521 s, ν(M—N) 571 s.

Nickel (II) complex

This was prepared similarly from $Ni(AcO)_2$ $4H_2O$ (0.250 g, 7.5×10^{-4} mol) and OBPIMP (0.500 g, 1.8×10^{-3} mol/unit) in THF (yield 15%).

Calcd. for OBPIMP-Ni: M, 17.64. Found: M, 12.05. UV–vis (λ_{max}): 208, 237, 281, 341, and 388 nm. FTIR (KBr, cm^{-1}): ν(O—H) 3137 s, ν(C—H aryl) 3050 m,

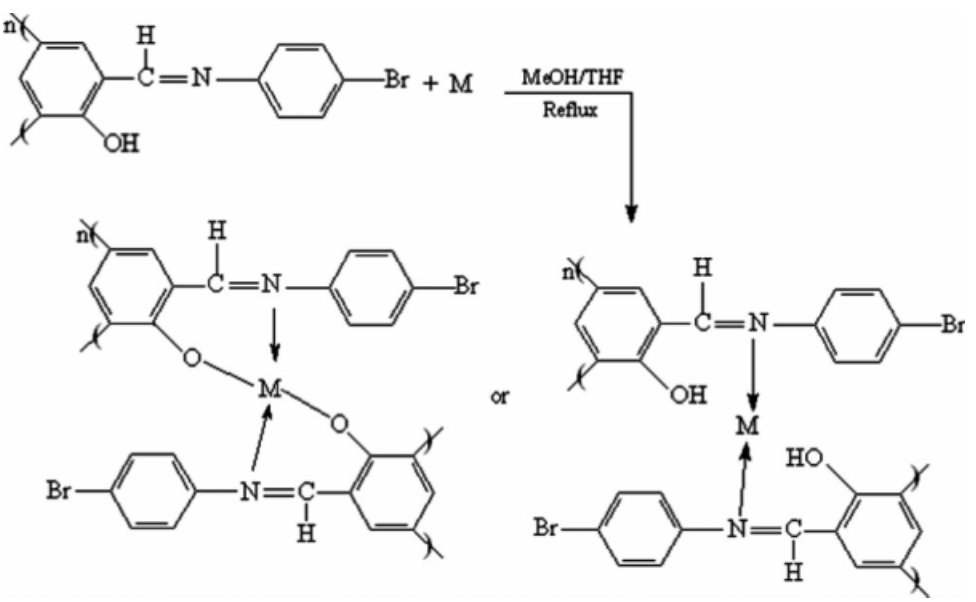

Scheme 2 Syntheses of oligomer-metal complexes.

v(C═N) 1614 s, v(aromatic, C—O) 1282 s, v(C—Br) 828 s, v(aromatic, C═C) 1533, 1416 m, v(M—O) 517 s, v(M—N) 595 s.

Copper (II) complex

This was prepared similarly from $Cu(AcO)_2$ H_2O (0.200 g, 5.9×10^{-4} mol) and OBPIMP (0.400 g, 1.46×10^{-3} mol/ unit) in THF (yield 60%).

Calcd. for OBPIMP-Cu: M, 18.83. Found: M, 16.25. UV–vis (λ_{max}): 206, 238, 280, 341, and 384 nm. FTIR (KBr, cm^{-1}): v(O—H) 3446 s, v(C—H aryl) 3048 m, v(C═N) 1607 s, v(aromatic, C—O) 1181 s, v(C—Br) 831 s, v(aromatic, C═C) 1583, 1533, 1483, 1464 m, v(M—O) 530 s, v(M—N) 589 s.

Characterization techniques

The infrared and ultraviolet-visible spectra were measured by Perkin Elmer BX II and Perkin Elmer Lambda 25, respectively. Elemental analysis was carried out with a Carlo Erba 1106. The FTIR spectra were recorded on KBr discs (4000–350 cm^{-1}). UV–vis spectra of BPIMP, OBPIMP, OBPIMP-Co, OBPIMP-Ni, and OBPIMP-Cu were determined by using MeOH and DMSO. BPIMP and OBPIMP were characterized by ^{1}H-NMR and ^{13}C-NMR spectra (Bruker Avance DPX-400 and 100.6 MHz, respectively) recorded at 25°C using deuterated DMSO as a solvent. Tetramethylsilane was used as internal standard. Thermal data were obtained by using a Perkin-Elmer Diamond Thermal Analysis system. The TGA-DTA measurements were made between 15 and 1000°C (in N_2, 10°C/min). The number-average molecular weight (M_n), weight-average molecular weight (M_w), and polydispersity index (PDI) were determined by SEC (Shimadzu, Japan) with a Macherey-Nagel (Germany) (100 Å and 7-nm diameter loading material) 7.7 mm i.d.x 300 mm columns, DMF/MeOH eluent (v/v 4/1, 0.4 mL min^{-1}), polystyrene standards, and a refractive index detector at 30°C. Metal analyses of oligomer-metal complex compounds were carried out by AAS Shimadzu 6200 in a solution prepared by decomposition of the oligomer-complexes with HNO_3 followed by dilution with deionized water. The magnetic moments of oligomer-metal complexes were measured by a MK-1 model Gouy Balance (Christison Scientific Equipment) at room temperature.

RESULTS AND DISCUSSION

The investigation of synthesis conditions of OBPIMP

Because of the electron donating effect of the azomethine group, 2-[(4-bromophenylimino)methyl]phenol is polymerized by air and NaOCl oxidants the various temperatures and reaction times in an aqueous alkaline medium. The oxidative polycondensation reaction conditions of BPIMP with NaOCl in an aqueous alkaline medium are given in Table I. The oxidative polycondensation reaction of BPIMP was immediately formed in an aqueous alkaline solution and the solution turned into brown by adding oxidants such as NaOCl and air. The yield of OBPIMP was 88% at the oxidative polycondensation reaction conditions such as $[BPIMP]_0 = 0.03$, $[KOH]_0 = 0.06$, and $[NaOCl]_0 = 0.03$ mol/L, at 50°C for 2 h. Under the same conditions, the yield of OBPIMP decreased with increasing of the reaction times and this value was found to be 48% (see Table I, Sample No.12). Both, the yield of OBPIMP affected from increasing of initial concentration of KOH. The oxidative polycondensation reaction conditions of BPIMP with air oxidant in an aqueous alkaline medium are given in Table I. The yield of OBPIMP was 67% at the reaction conditions such as $[BPIMP]_0 = 0.03$, $[KOH]_0 = 0.06$ mol/L, and 8.5 L/h flow rate of air, at 50°C for 5 h. Under the same conditions, the yield of OBPIMP decreased with increasing of the reaction times and this value found to be 30% (see Table I, Sample No. 25). According to these results, NaOCl oxidant was more effective than air as the oxidative polycondensation reaction initiator.

Solubility

The oxidative polycondensation product of BPIMP synthesized by NaOCl and air oxidants in an aqueous alkaline medium and product was at black solid powder form. OBPIMP was soluble in conc. H_2SO_4, THF, DMF, DMSO, and acetone. However, OBPIMP was poorly soluble in toluene, benzene, and chlorinated solvents such as $CHCl_3$ and CCl_4. OBPIMP was insoluble in aliphatic hydrocarbons such as heptane and hexane. Oligomer–metal complexes were obtained from the reaction of OBPIMP with Co^{+2}, Ni^{+2}, and Cu^{+2} acetates salts. As expected the new oligomer-metal complexes were soluble in DMSO and DMF. The complexes were broken by both an aqueous alkaline solution and concentrated H_2SO_4.

Structure of OBPIMP

The M_n and M_w of OBPIMP were calculated according to a polystyrene standard calibration curve from SEC measurements. When the NaOCl was used as oxidant, the M_n, M_w, and PDI values of OBPIMP were found to be 1700, 2120 g mol^{-1}, and 1.25, respectively. The M_n, M_w, and PDI values of OBPIMP were found to be 1940, 2230 g mol^{-1}, and 1.15, respectively, with air as the oxidant. This oligomer was contained about 6 and 7 repeating units. According to PDI values, they showed narrow molecular weight distribution.

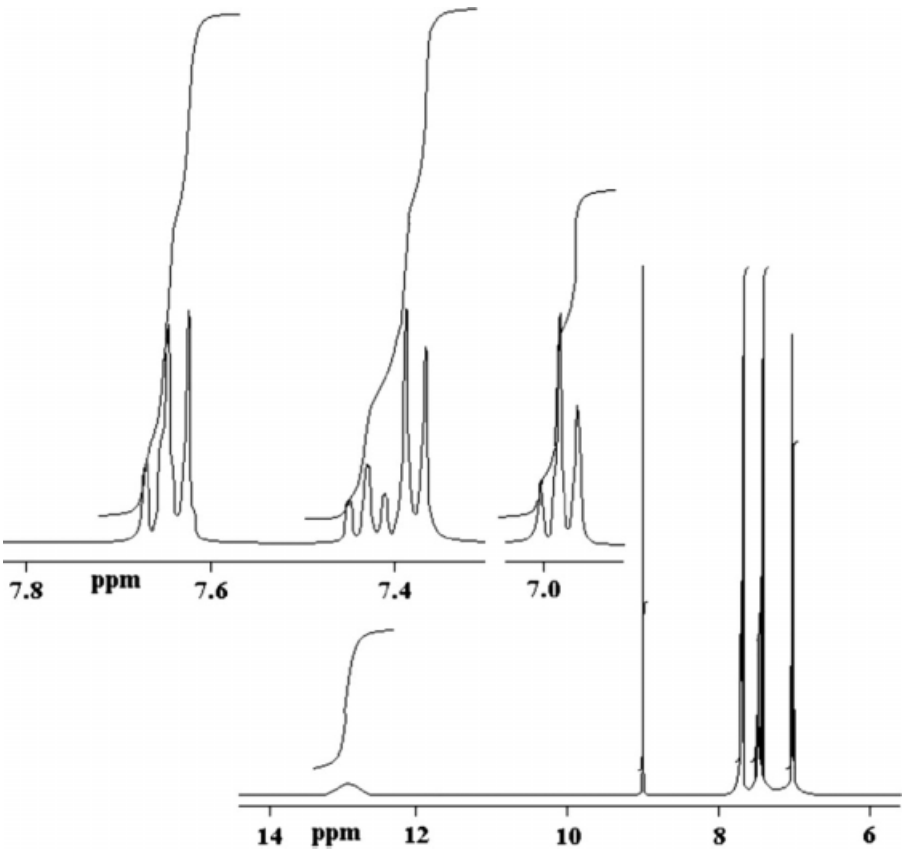

Figure 1 ^{1}H-NMR spectrum of 2-[(4-bromophenylimino)methyl]phenol.

The characteristic peaks of the functional groups were observed in the FTIR spectrum of OBPIMP. Phenyl-OH group at 3435 cm^{-1}, aromatic —CH groups at 3067 cm^{-1}, azomethine (—CH=N) group at 1612 cm^{-1}, C—Br 755 cm^{-1} and —C=C double bonds at 1586, 1485, 1458 cm^{-1}. The electronic spectra of BPIMP and OBPIMP were recorded in methanol and DMSO, respectively. The λ_{max} values of BPIMP was observed at 211, 230, 273, 320, and 341 nm. K band belong to —OH and azomethine groups of BPIMP was observed at 230 and 320 nm, respectively. B and R bands of BPIMP were observed at 273 and 341 nm. R band of —CH=N group of BPIMP was observed at 341 nm. The same bands were observed at 240, 288, 330, and 354 nm at the UV–vis spectrum of OBPIMP. K bands belong to =OH and azomethine groups of OBPIMP were observed in 240 and 330 nm, respectively. R band of —CH=N group of OBPIMP was observed at 354 nm. In the oligomer-metal complexes, the low intensity bands in the 450–550 nm range are consistent with d→d transitions of the metal ions.

The synthesis of polymers with azomethine structure containing 1, 5-naphthyl or 1, 4-phenyl moieties through polycondensation of some dialdehydes with diamines has been reported in the literature.[18] Both monomers and polymers have been characterized by FTIR and ^{1}H-NMR techniques. Thermo gravimetric analyses had been made for all the synthesized polymers to study their thermal behaviors.[28]

To identify the structures of BPIMP and OBPIMP, the ^{1}H-NMR and ^{13}C-NMR spectra were recorded in DMSO-d_6 and are given in Figures 1–3. The signals of —OH and —CH=N groups of BPIMP and OBPIMP were observed in 12.40, 8.90, 12.82, and 8.97 ppm, respectively. According to ^{13}C-NMR, the peak values of C1 and C2 observed in 163.54 and 116.35 ppm in the monomer and 164.46 and 118.42 ppm in the oligomer, respectively. These values are in agreement with the theoretically calculated peak position for *ortho* linkages on the ring.[29] The oxyphenylene are involved in the formation of free radicals leading to oligomer formation and they appeared to be involved in bond formation. Thus, the phenyl rings in the oligomer seems to be linked primarily at ortho and oxyphenylene. The ^{1}H-^{13}C-NMR results showed that the polymerization of BPIMP proceeded by C—C and C—O coupling from ortho position according to —OH group and oxyphenylene, respectively. The FTIR spectral data of the BPIMP and OBPIMP confirm the results of the ^{1}H-NMR spectra. Because of C—C coupling system, the new peak observed in 121.93 ppm in the ^{13}C-NMR spectra of oligomer.

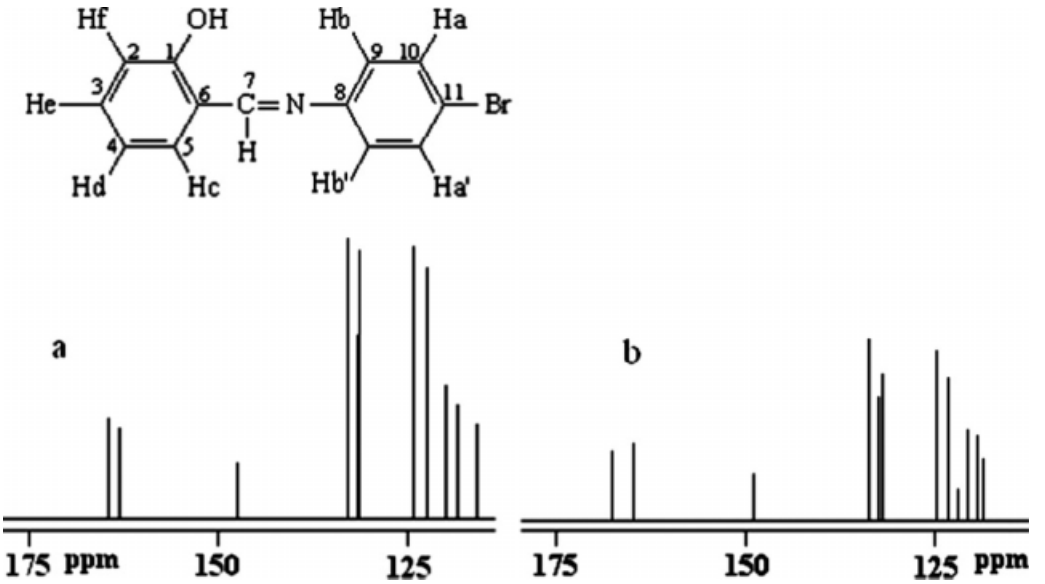

Figure 2 ^{13}C-NMR spectrum of BPIMP (a) and BPIMP (b).

Thermal analyses of OBPIMP and oligomer-metal complexes

DTA and TG analyses of BPIMP, OBPIMP, OBPIMP-Cu, OBPIMP-Ni, and OBPIMP-Co compounds were measured under an N_2 atmosphere in the temperature ranges of 15–1000°C and traces are given in Figures 4–8, respectively. The initial degradation temperature, 50% and 99.45% weight loss of BPIMP was found to be 239, 280, and 1000°C, respectively. According to DTG curve, thermal degradation of BPIMP completed at 320°C. The degradation of OBPIMP started at 216°C. OBPIMP broke up at the high rate between 250 and 300°C. The respective

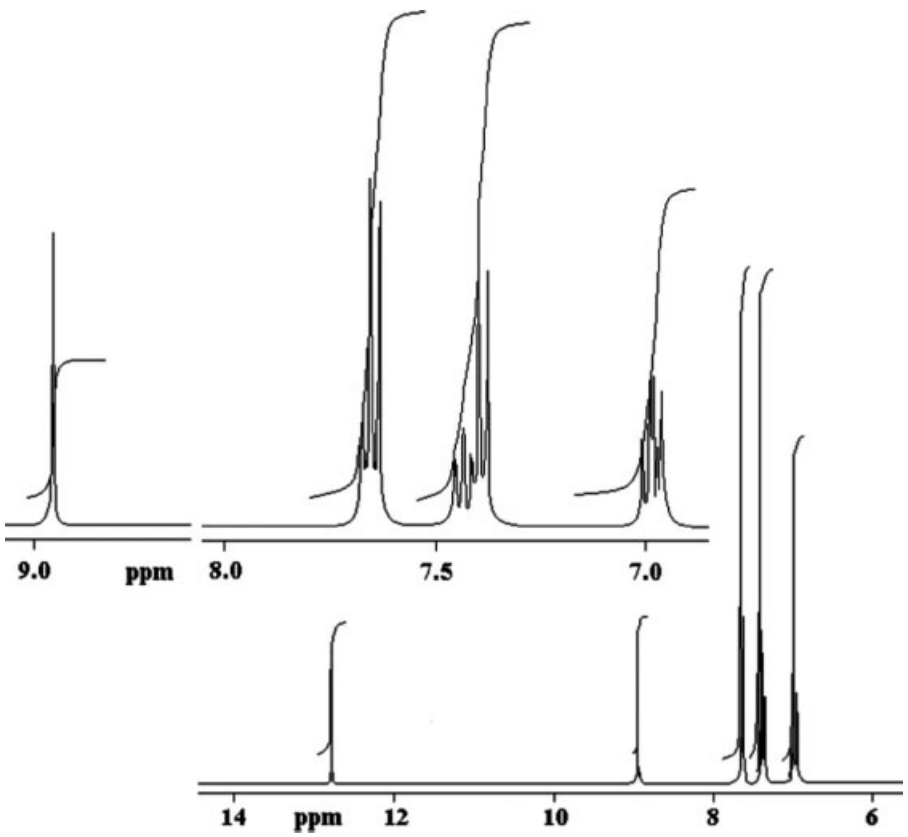

Figure 3 ^{1}H-NMR spectrum of oligo-2-[(4-bromophenylimino)methyl]phenol.

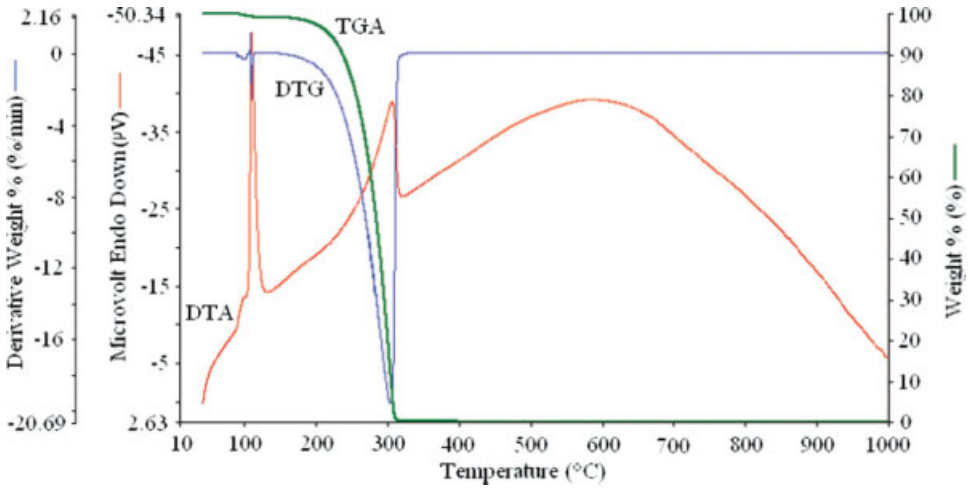

Figure 4 TGA-DTG-DTA curves of BPIMP. [Color figure can be viewed in the online issue, which is available at www.interscience.wiley.com]

weight loss of OBPIMP was found to be 93% at 1000°C. Because of C—O coupling formation, initial degradation temperature of oligomer was lower than monomer according to TGA measurements. C—O coupling system has been degradated at lower temperature than C—C. The carbonaceous residues of OBPIMP-Co, OBPIMP-Ni, and OBPIMP-Cu complexes were found to be 40.20, 25.77, and 40.70% at 1000°C, respectively. Fifty percent of weights of OBPIMP-Co, OBPIMP-Ni, and OBPIMP-Cu were lost at 540, 500, and 450°C, respectively. Metal complexes of OBPIMP demonstrated higher thermal stability than the monomer and oligomer. The initial degradation temperatures of OBPIMP-Co, OBPIMP-Ni, and OBPIMP-Cu were found to be 244, 298, and 257°C, respectively. Total weight losses of Co^{+2}, Ni^{+2}, and Cu^{+2} complexes of OBPIMP were 59.80%, 74.23%, and 59.30%, respectively, at 1000°C. Exothermic process of Cu^{+2}, Ni^{+2}, and Co^{+2} complexes of OBPIMP started between 300 and 650°C and T_{max} values were 400, 625, and 350°C, respectively. The initial and final temperatures and total mass losses for each step in the thermal decomposition of complexes are given in Table II, together with temperatures of greatest rate of decomposition (DTG_{max}). BPIMP shows a decomposition stage in the temperature range of 185 and 329°C with a 98.95% weight loss. The DTA profile exhibited two endothermic thermal effects at 109 and 328°C. First peak corresponds to the melting point of BPIMP, while the second, at 321°C peak corresponds to the decomposition of BPIMP. From the TGA curve for OBPIMP, it seems that the sample decomposes in one stage over the temperature range 180–308°C. DTA profile shows two exothermic effects. The first, at 111°C corresponding to the melting point of OBPIMP, whereas the second, at 274°C corresponding the decomposition of the complex. Also, according to

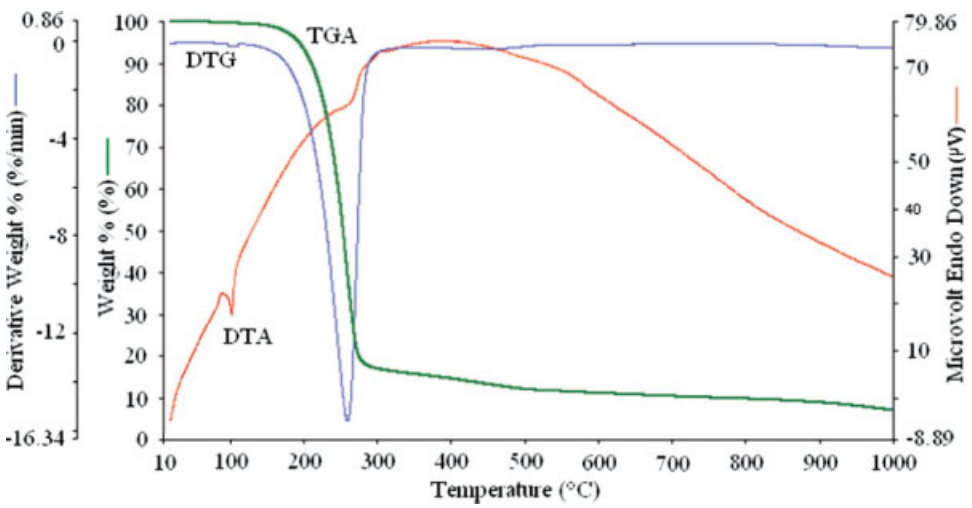

Figure 5 TGA-DTG-DTA curves of OBPIMP. [Color figure can be viewed in the online issue, which is available at www.interscience.wiley.com]

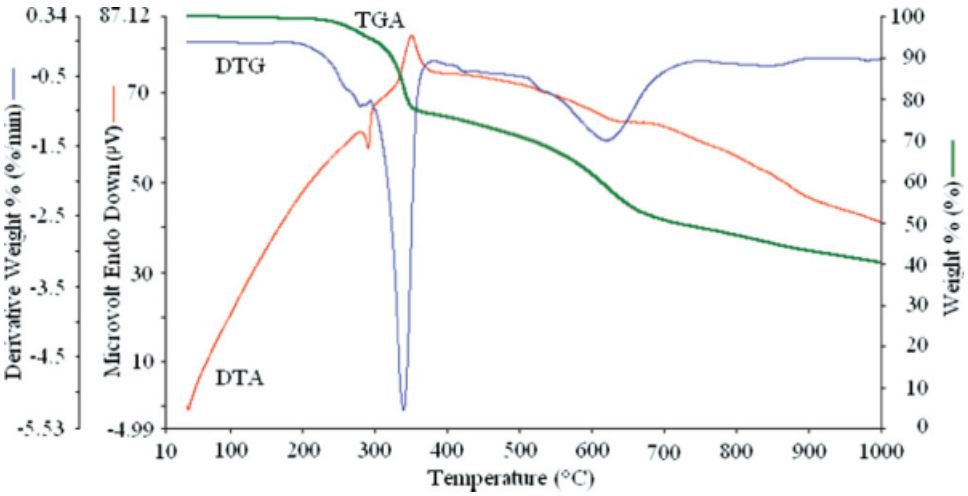

Figure 6 TGA-DTG-DTA curves of OBPIMP-Co. [Color figure can be viewed in the online issue, which is available at www.interscience.wiley.com]

TG analysis, although the initial degradation temperature of OBPIMP was lower than BPIMP, it was more stable than BPIMP due to the long conjugated band systems. OBPIMP-Cu demonstrated higher thermal stability than monomer, oligomer, and other oligomer-metal complexes. It was found that the thermal stabilities of the monomer, oligomer and oligomer-metal complexes follow as: OBPIMP-Cu > OBPIMP-Co > OBPIMP > BPIMP > OBPIMP-Ni.

Kinetic and thermodynamic parameters

TGA experiments could be performed to determine thermal behavior of BPIMP, OBPIMP and OBPIMP-Cu, OBPIMP-Co, and OBPIMP-Ni and to suggest degradation processes and kinetic parameters. The CR, vK, MC methods were used for the kinetic analysis. These methods are based on a single heating rate (10 °C, min^{-1}). From the TGA curves, the reaction order, n, the apparent activation energies of thermal decomposition, E_a, entropies, ΔS^*, enthalpy change, ΔH^*, free energy change, ΔG^*, pre-exponential factor, A, and the linearization curves of the thermal degradation of all materials have been elucidated by the methods mentioned earlier. The obtained results are given in Table III.

According to Coats and Redfern method, the plot of ln $[g(\alpha)/T^2]$ versus $1/T$ gives straight line with slope equals to $-E_a/R$. The apparent activation energies of thermal decomposition of each decomposition stage of BPIMP, OBPIMP, and oligomer-metal complexes were calculated from Figures 9 and 10.

Figures 11 and 12 show Arrhenius plots determined by the method of van Krevelen in nitrogen for weight loss thermograms of 10°C min^{-1}. The apparent activation energies of thermal decomposition

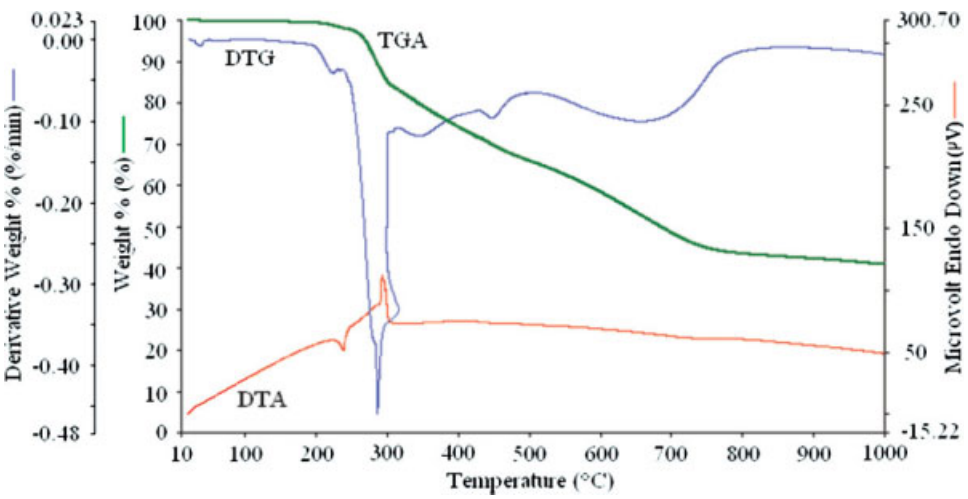

Figure 7 TGA-DTG-DTA curves of OBPIMP-Cu. [Color figure can be viewed in the online issue, which is available at www.interscience.wiley.com]

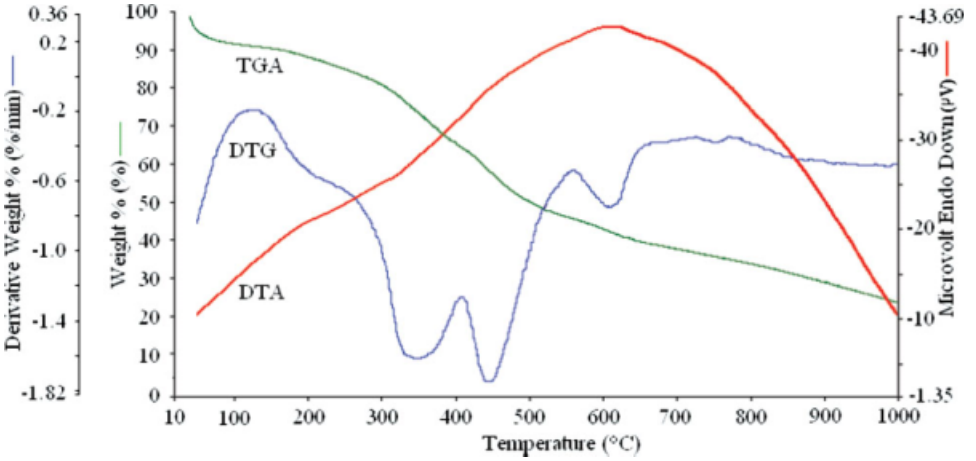

Figure 8 TGA-DTG-DTA curves of OBPIMP-Ni. [Color figure can be viewed in the online issue, which is available at www.interscience.wiley.com]

TABLE II
TG, DTG, and DTA Data for the Monomer, Oligomer, and Oligomer-Metal Complexes

Compound	Step	DTA peak (°C)	DTG_{max} (°C)	Temperature range (°C)	DTA	% Carbine residue at 1000°C
BPIMP	I	109, 328	324	185–329	Exo, exo	
	Residue	>329				1.05
OBPIMP	I	111, 274	274	180–308	Endo, endo	
	Residue	>308				18.05
OBPIMP-Co	I	223, 282	271	202–317	Endo, exo	17.03
	II		639	359–786		40.21
	Residue	>786				42.76
OBPIMP-Cu	I	281, 338	328	229–353	Exo, endo	20.66
	II	609	609	353–724	exo	38.11
	Residue	>724				41.23
OBPIMP-Ni	I		361	257–383		38.19
	II		467	383–6269		36.67
	Residue	>626				25.14

TABLE III
The Thermodynamic and Kinetic Parameters Obtained by the Different Methods

Materials	Stage	Methods	n	E_a	ln A	ΔS^*	ΔH^*	ΔG^*	r
BPIMP	I	vK	0.3	86.89	19.17	−91.27	81.92	136.4	0.99736
		MC	0.5	85.54	22.61	−62.71	80.57	118.0	0.99709
		CR	0.5	76.25	13.95	−134.6	71.28	151.6	0.99665
OBPIMP	I	MC	0.9	105.4	28.07	−16.51	100.9	109.9	0.99701
		vK	0.9	107.4	28.71	−11.20	102.9	109.0	0.99665
		CR	0.9	96.31	19.53	−87.52	91.76	139.6	0.99654
OBPIMP-Co	I	MC	0.1	47.22	14.37	−130.3	42.69	113.6	0.99656
		vK	0.2	45.14	10.11	−165.8	40.61	130.8	0.99519
		CR	0.2	39.84	5.811	−201.6	35.31	145.0	0.99439
	II	vK	0.8	39.29	6.052	−203.9	31.70	217.6	0.99773
		MC	0.6	35.91	9.694	−173.6	28.32	186.6	0.99655
		CR	0.9	31.34	0.693	−248.4	23.75	250.3	0.98027
OBPIMP-Cu	I	MC	0.5	110.2	26.89	−27.17	105.2	121.6	0.99899
		vK	0.5	112.3	24.53	−46.79	107.3	135.4	0.99809
		CR	0.5	100.2	18.16	−99.75	95.29	155.2	0.99876
	II	MC	0.9	76.51	15.48	−125.1	69.17	179.5	0.99528
		CR	1.0	65.36	6.327	−201.3	57.96	235.5	0.99347
		vK	0.1	78.05	10.81	−164.0	70.71	215.3	0.99055
OBPIMP-Ni	I	MC	0.7	65.18	14.41	−131.3	59.90	143.1	0.99756
		vK	0.8	60.83	12.08	−150.7	55.55	151.1	0.99568
		CR	0.8	62.04	6.476	−197.3	56.76	181.9	0.98792
	II	vK	0.4	57.79	12.59	−147.7	51.63	160.9	0.99701
		MC	0.4	58.95	15.89	−120.3	52.79	141.8	0.99567
		CR	0.4	48.81	6.823	−195.7	42.65	187.5	0.99421

E_a is measured in kJ mol^{-1}, A in s^{-1}, ΔS^* in kJ mol^{-1}, ΔH^* in kJ mol^{-1}, ΔG^* in kJ mol^{-1}, r is thecorrelation coefficients of the linear plot, and n is the order of reaction.

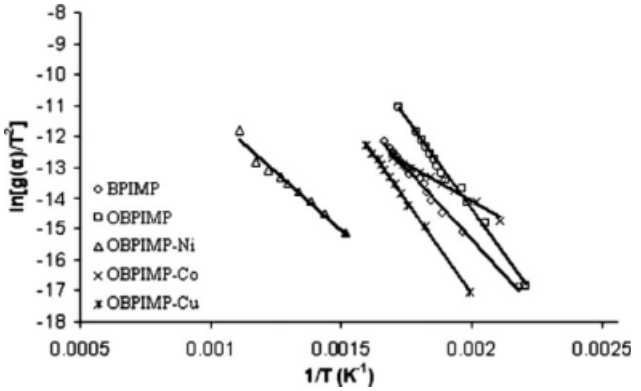

Figure 9 CR plots of the first decomposition stage of BPIMP, OBPIMP, OBPIMP-Ni, OBPIMP-Co, and OBPIMP-Cu.

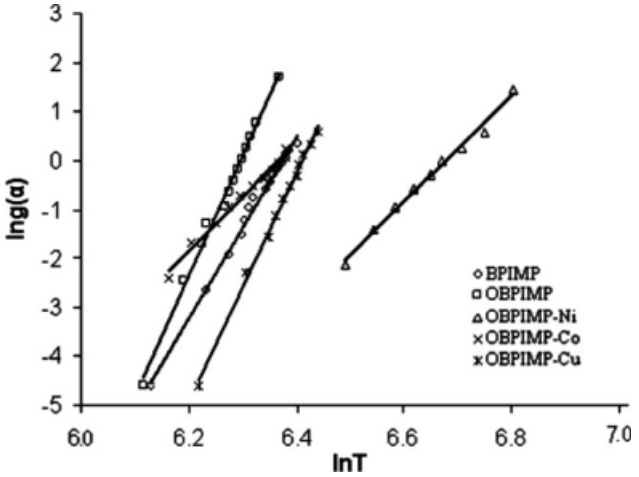

Figure 11 vK plots of the first decomposition stage of BPIMP, OBPIMP, OBPIMP-Ni, OBPIMP-Co, and OBPIMP-Cu.

can calculate from slopes of the ln $g(\alpha)$ against ln T plot. Finally, as seen in Figures 13 and 14 in cases of MC method the apparent activation energies of thermal decomposition were calculated from the slopes of plots.

For all methods, determination of the pre-exponential factor and reaction order is possible from the expression of $g(\alpha)$ in eq. (3) and $n \neq 1$:

$$g(\alpha) = \frac{1 - (1 - \alpha)^{1-n}}{1 - n}$$

The linearization of obtained curves of BPIMP, OBPIMP, and oligomer-metal complex compounds using the methods mentioned above were presented in Figures 9–14. Moreover, Table III summarizes the thermodynamic and kinetic parameters obtained by the five different methods examined in this study. The results are in good agreement with the values obtained from all of them. The results indicate that the values of all methods are comparable. As seen in Table III, the values of correlation coefficients of linearized curves of BPIMP, OBPIMP, and oligomer-metal complexes are approximately 1.00. The kinetic data obtained by different methods agree with each other. The enthalpy change ΔH^*, entropy change ΔS^*, and the free energy change ΔG^*, of all material were calculated using the following relations[30]:

$$\Delta S^* = 2.303 \log\left(\frac{Ah}{kT}\right) R$$

$$\Delta H = E_a - RT$$

$$\Delta G^* = \Delta H - T\Delta S^*$$

where h is the Planck constant and T is the temperature, and A is the pre-exponential factor. The calculated thermodynamic parameters were reported in Table III.

It was found that the activation energy of the oligomer-metal complexes follow the order OBPIMP-

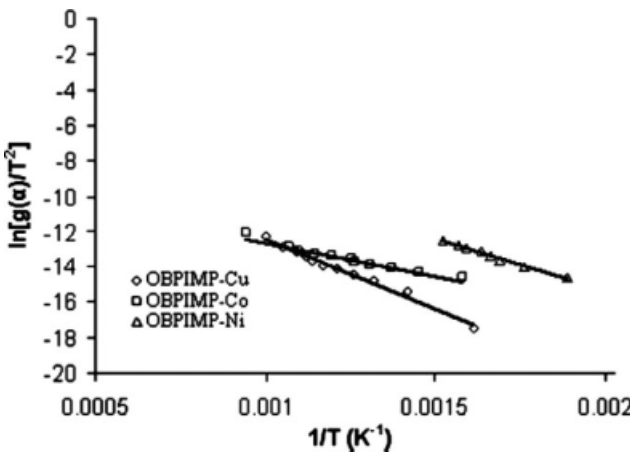

Figure 10 CR plots of the second decomposition stage of OBPIMP-Cu, OBPIMP-Co, and OBPIMP-Ni.

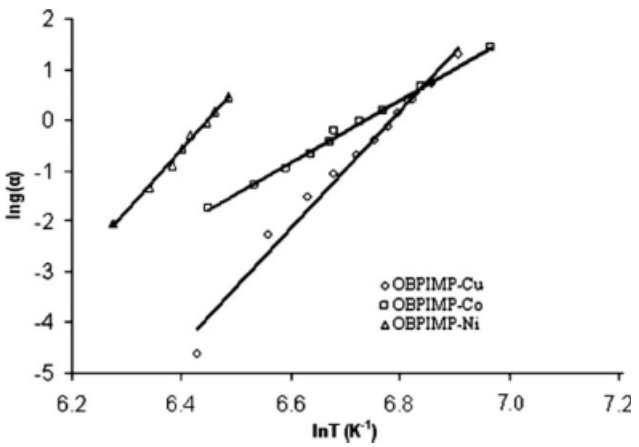

Figure 12 vK plots of the first decomposition stage of OBPIMP-Cu, OBPIMP-Co, and OBPIMP-Ni.

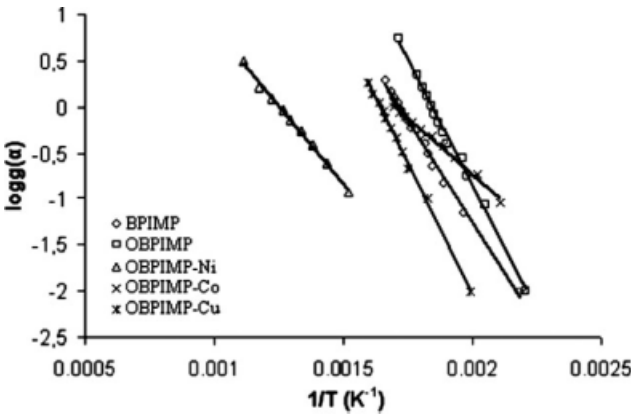

Figure 13 MC plots of the first decomposition stage of BPIMP, OBPIMP, OBPIMP-Ni, OBPIMP-Co, and OBPIMP-Cu.

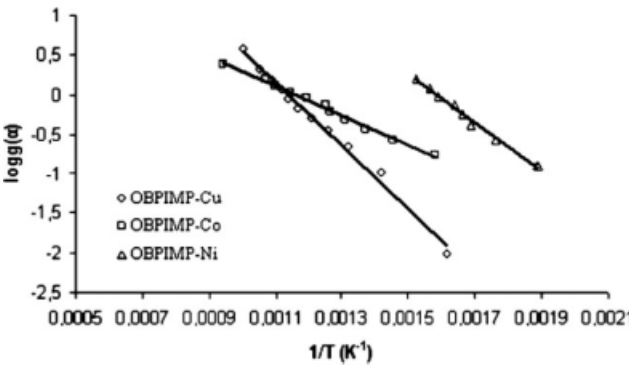

Figure 14 MC plots of the first decomposition stage of OBPIMP-Cu, OBPIMP-Co, and OBPIMP-Ni.

Cu > OBPIMP-Ni > OBPIMP-Co. The same order is also true for the second decomposition stage. The apparent activation energy of thermal decomposition and Gibbs free energy of the complexes also increase with increasing of atomic number in the 3rd series of the d-block elements. The kinetic parameters had been calculated from non-isothermal data

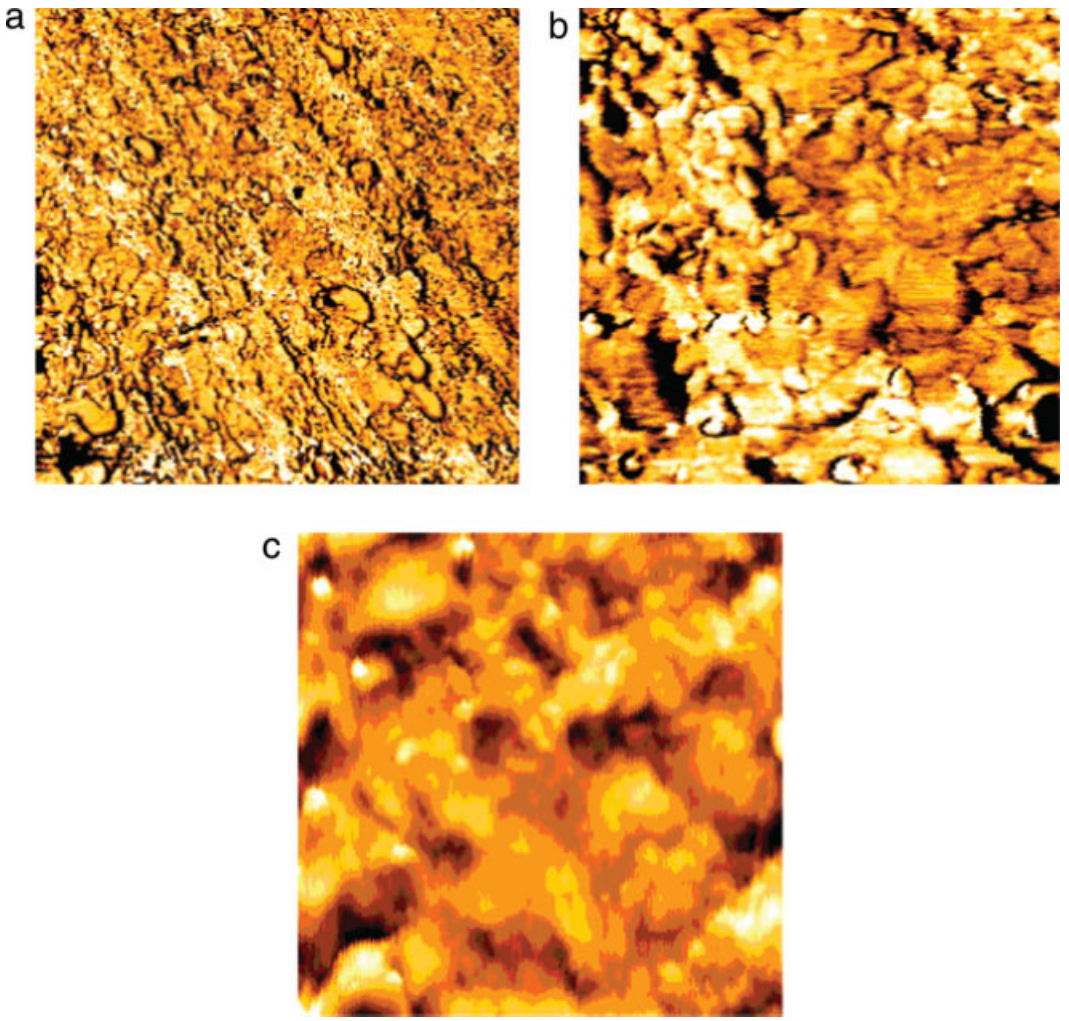

Figure 15 Atomic force microscopy (AFM) photographs of BPIMP. [Color figure can be viewed in the online issue, which is available at www.interscience.wiley.com]

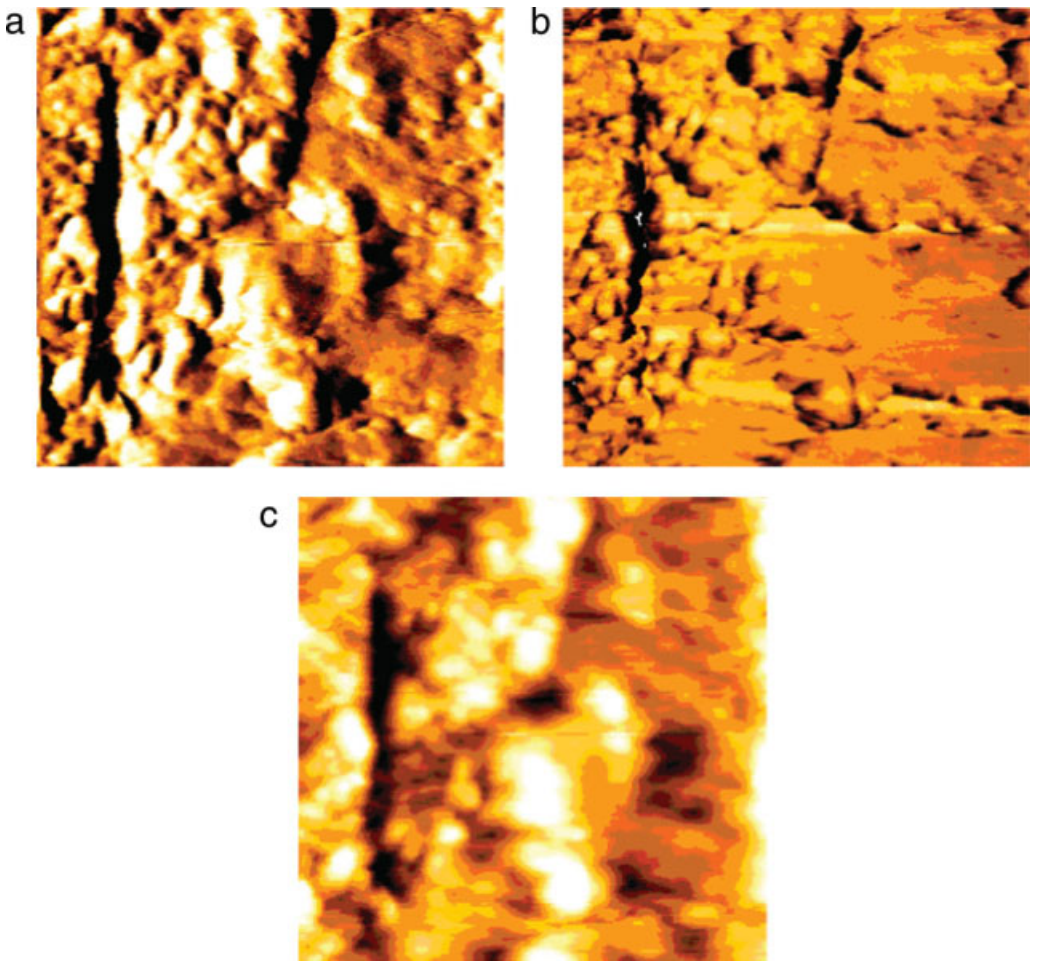

Figure 16 Atomic force microscopy (AFM) photographs of OBPIMP. [Color figure can be viewed in the online issue, which is available at www.interscience.wiley.com]

corresponding to thermal and thermo-oxidative degradation of polymers and polymeric materials.[31,32]

Surface Morphologies of monomer and oligomer

The surface morphologies of monomer and oligomer were studied by atomic force microscopy (AFM) (Veeco, Digital Instruments CP-II SPM, Scanning scopes are 1 μm). Micrographs of the samples are shown in Figures 15 and 16. It is seen from the AFM micrographs of the samples that it has an almost uniform surface and they the topological surface structures are different. Also, in structure, voids have been consistent, which are probably due to applied pressure. Figures 15(a–c) demonstrated amplitude, phase and topography modes, respectively, for monomer. In topography mode of the monomer [Fig. 15(c)] seems homogeneous. Figure 16(a–c) demonstrated amplitude, phase and topography modes, respectively, for the oligomer. Figure 16(a,c) present white toroidal zones on both pictures. In phase mode of the oligomer [Fig. 16(b)] seems homogeneous, whereas Figure 16(a,c) shows an increase of white parts corresponding to a different chemical structure of the heightened part.

Geometrical structures of oligomer-metal complexes

In this part, we would like to elucidate the important role played by magnetic and FTIR spectra in determining the geometrical structures of the above investigated metal chelates. Most of the band shifts observed at the wave number region 1282–1172 cm^{-1} is in agreement with the structural changes observed in the molecular carbon skeleton after complexation, which cause some important changes in (C—C) bond lengths. The ν(M—N) band for the ligand complexes are appeared in the wave number range 571–595 cm^{-1}. New sharp peaks, small or broad intensities observed in the wave number range 517–530 cm^{-1} are assigned to the M—O vibration. The magnetic moment value of Cu^{+2} complex was found to be 2.15 B.M and an indicative of the

appearance of the copper complex in a square planar geometry.[33] Ni^{+2} and Co^{+2} complexes are diamagnetic. The diamagnetic nature coupled with elemental analysis data suggests a tetrahedral environment of chelating ligands around the metal ions.[34]

CONCLUSION

The structures of BPIMP and OBPIMP were characterized by chemical and spectral analyses. The spectral analyses such as ^{1}H and ^{13}C-NMR have demonstrated to unite from ortho carbon and oxyphenylene of phenol ring each other of formation oligomers from oxidative polycondensation of BPIMP. According to molecular weight distribution, the M_n, M_w, and PDI values of OBPIMP were found to be 1700, 2120 g mol^{-1}, and 1.25 and 1940, 2230 g mol^{-1}, and 1.15, for NaOCl and air oxidants, respectively. The yield of OBPIMP was found to be 88% and 67% by NaOCl and air oxidants, respectively. NaOCl was more reactive than air for the oxidative polycondensation reaction of BPIMP. According to TG analyses, OBPIMP, OBPIMP-Co, OBPIMP-Ni and OBPIMP-Cu complexes lost about 93.04%, 59.80, 74.23, and 59.30% of weights at 1000°C, respectively. According to TGA results, the highest residue observed at the OBPIMP-Cu complex. That is, OBPIMP-Cu complex has higher thermal stability than OBPIMP-Ni and OBPIMP-Co complexes. The reaction order, n, the activation energies of thermal decomposition, E_a, entropies, ΔS^*, enthalpy change, ΔH^*, free energy change, ΔG^*, pre-exponential factor, A, and the linearization curves of the thermal degradation of monomer, oligomer and oligomer-metal complexes were calculated by CR, MC, and vK methods from the TGA curves.

References

1. Marcu, M.; Cazacu, M.; Vlad, A.; Racles, C. Appl Organomet Chem 2003, 17, 693.
2. Cazacu, M.; Marcu, M.; Vlad, A.; Toth, A.; Racles, C. J Polym Science Part A: Polym Chem 2003, 41, 3169.
3. Racles, C.; Cozan, V.; Cazacu, M.; Földes, E.; Sajo, I. High Perform Polym 2002, 14, 397.
4. Marin, L.; Cozan, V.; Bruma, M.; Grigoras, V. C. Eur Polym J 2006, 42, 1173.
5. Shukla, U.; Rao, K. V.; Rakshit, A. K. J Appl Polym Sci 2003, 88, 153.
6. Diaz, F. R.; Moreno, J.; Tagle, L. H.; East, G. A.; Radic, D. Synth Met 1999, 100, 187.
7. Sun, S. J.; Chang, T. C.; Li, C. H. Eur Polym J 1993, 29, 951.
8. Aly, K.; Khalaf, A. A.; Alkskas, I. A Polym J 2003, 39, 1035.
9. El-Shekeil, A.; Al-Aghbari, S. Polym Int 2004, 53, 777.
10. Grigoras, M.; Catanescu, O. C.; Colotin, G. Macromol Chem Phys 2001, 202, 2262.
11. Kaya, İ.; Koyuncu, S. Mater Lett 2006, 60, 1922.
12. Scriven, E. F. V. Chem Soc Rev 1983, 12, 129.
13. Ragimov, A. V.; Mamedov, B. A.; Yasamova, S. Y. Polym Int 1997, 43, 343.
14. Bolto, B. A. J Macromol Sci Chem 1980, 14, 107.
15. Cosellato, U.; Vigato, P. A.; Vidali, M. Coordinat Chem Rev 1981, 36, 183.
16. Walter, C. I.; Anderson, H. L.; Sanders, J. K. J Chem Soc Commun 1964, 4, 58.
17. Yousef, U. S. Eur Polym J 2000, 36, 1629.
18. Patel, M. N.; Patil, S. H. J Macromol Science: Pure Appl Chem 1981, 16, 1429.
19. Kaya, İ.; Yildirim, M. Eur Polym J 2007, 43, 127.
20. Kaya, İ.; Koça, S. Polymer 2004, 45, 1743.
21. Kaya, İ.; Bilici, A. J Macromol Sci Part A: Pure Appl Chem 2006, 43, 719.
22. Keattch, C. J.; Dollimore, D. An Introduction to Thermogravimetry; Wiley: London, 1975; p. 144.
23. Coats, A. W.; Redfern, J. P. Nature 1964, 201, 68.
24. Doyle, C. D. J Appl Polym Sci 1970, 6, 1033.
25. MacCallum, J. R.; Tanner, J.Eur Polym J 1951, 30, 253.
26. Van Krevelen, D. W.; van Heerden, C.;Huntjons, F. J. Fuel 1961, 5, 285.
27. Kaya, İ.; Karayiğitler, H.; Özdemir, E. Int J Polym Anal Character 2006, 11, 271.
28. Catanescu, O.; Grigoras, M.; Colotin, G.; Dobreanu, A.; Hurduc, N.; Simionescu, C. I. Eur Polym J 2001, 37, 2213.
29. Ayyagari, M. S.; Marx, K. A.; Tripathy, S. K.; Akkara, J. A.; Kaplan, D. L. Macromolecules 1995, 28, 5192.
30. Mahfouz, R. M.; Al-Farhan, K. A.; Hassen, G. Y.; Al-Wassil, A. I.; Alshehri, S. M.; Aml, A.; Al-Wallan, A. A. Synth React Inorg Met-Org Chem 2002, 32, 489.
31. Budrugeac, P. Polym Degrad Stab 2005, 89, 265.
32. Vyazovkin, S.; Sbirrazzuoli, N. Macromol Rapid Commun 2006, 27, 1515.
33. Cotton, F. A.; Wilkinson, G. Advanced Inorganic Chemistry, 3th ed.; Wiley: New York, 1972; pp 875–901.
34. Kaliyappan, T.; Raman, A.; Kannan, P. J Macromol Sci Part A: Pure Appl Chem 1999, 36, 517.